Numerical study on flow topology and hemodynamics in tortuous coronary artery with symmetrical and asymmetrical stenosis

Jianfei Song, Smaïne Kouidri, Farid Bakir

Numerical study on flow topology and hemodynamics in tortuous coronary artery with symmetrical and asymmetrical stenosis

Jianfei Song[a,b,c], Smaine Kouidri[a,b,*] and Farid Bakir[a]

[a]*LIFSE, Arts et Métiers, 151 boulevard de l'Hopital, 75013 Paris, France*

[b]*LIMSI, CNRS, Université Paris-Saclay, Bât. 508, Rue John Von Neumann, Campus Universitaire, F-91405 Orsay Cedex, France*

[c]*Tianjin Key Laboratory of Refrigeration Technology, Tianjin University of Commerce, Tianjin, China*

*Corresponding author: Smaine Kouidri

E-mail: smaine.kouidri@limsi.fr

Acknowledgements

This study was supported by China Scholarship Council. The authors would like to thank Doctor Blandine Maurel, vascular surgeon at Nantes Hospital for sharing her expertise on atherosclerosis.

Numerical study on flow topology and hemodynamics in tortuous coronary artery with symmetrical and asymmetrical stenosis

Abstract

Tortuosity in coronary artery has been found to be greatly related to the potential sites of stenosis in these last years. Many investigations have been carried out based on the tool of Computational Fluid Dynamics (CFD) mainly focusing on the influences of curved artery in blood flow. Within the limited investigations of coupling between stenosis and tortuosity, the stenosis has been considered to be located at the tortuous segment. However, with recent clinical studies, the case of stenosis occurred at non-tortuous segment before tortuosities has been confirmed which has not been paid enough attention yet. Therefore, the present study aims to investigate the disturbed streamlines and hemodynamics in curved and spiral artery considering symmetrical and asymmetrical stenosis upstream these tortuosities. Different stenosis severities, pulse rates and distances between stenosis and tortuosity as controlling parameters have been studied. The distribution of time averaged wall shear stress (TAWSS) and streamlines through tortuous segment have been displayed in order to determine the potential disease sites. Artery surface of TAWSS below critical value has been quantified as well to evaluate the risks of atherosclerosis. The results reveal that larger artery surface of TAWSS below critical value generally goes with smaller pulse rate, larger stenosis severity and distance between stenosis and tortuosity both for curved and spiral artery. However, exceptions were found in the cases of distance of 6 mm in curved artery with symmetrical stenosis and stenosis severity of 50% in spiral artery. Moreover, the spiral tortuosity tends to suppress the potential risks of atherosclerosis compared to curved tortuosity.

Keywords: Tortuous coronary artery; Wall shear stress; Hemodynamics; Flow topology; Computational Fluid Dynamics

1. Introduction:

Atherosclerosis as a chronic disease has been found to be responsible for 1/3 deaths in developed and developing countries [1, 2]. Narrowed artery will be observed due to the stenosis formation when disease happens. Numerous studies have been published to

elucidate the hemodynamic variations due to disturbed flow in stenotic artery [3, 4, 5, 6, 7]. In 2018, T. Sood et al. [8] demonstrated that varied pulse rates of blood flow greatly affect vortices formation downstream the stenosis. Increased pulse rate brings more disturbed flow downstream especially for asymmetric stenosis.

Arterial tortuosity is commonly found in human body especially in the left anterior descending coronary artery [9]. In the recent years the relationship between artery tortuosity and stenosis occurrence has caused great interest among researchers. Many studies have been carried out focusing on the curved artery [10, 11, 12]. M. Jarrahi et al. [13], M.R. Najjari et al. [14] and J.H. Siggers et al. [15] have experimentally studied the flow pattern in curved pipe to better understand the development of vortices structure through curvature. Recently numerical simulation as a research tool has been employed widely to investigate the physics of blood flow in the tortuous vessel [16]. The effects of morphological parameters of curvature on flow pattern and hemodynamics have been commonly discussed among the existing literature [17, 18, 19]. Wall shear stress (WSS) as a key hemodynamic indicator to potential atherosclerosis sites has been found to be strongly affected by tortuosity. X. Xie et al. [20] have shown that the increased curvature angle larger than 120^{o} contributes to a lower WSS zone. Through works in 2019 by A. Buradi et al. [21], it is found severe coronary tortuosity with small curvature radius, small distance between two curvatures and high angle of curvature will contribute to low WSS zones at inner wall downstream of tortuosity section.

Among these existing investigations up to now, many of them either mainly focus on the effect of vessel tortuosity or mainly focus on the effect of stenosis. The studies considering both stenosis and tortuosity are really limited. G.Y. Liu et al. [22], B.Y. Liu [23] and M. Biglarian et al. [24] have considered the stenosis located at curvature site and studied the flow topology and WSS distribution at inner wall and outer wall.

However, it should be noticed that through clinical investigations in 2018 [25], the stenosis located at the non-tortuous segment before the tortuosities has been confirmed and the hemodynamic variations affected by the interactions between stenosis and tortuosity still remain interesting in this case.

Therefore, in view of the literature, the present study aims to investigate the flow topology and hemodynamics through 3D tortuous artery model with symmetrical and asymmetrical stenosis located before the tortuous segment. As the previous studies focused mainly on the curved artery, in this study both curved and spiral tortuosity have been considered based on the clinical review by H.C. Han [26]. Different stenosis severities of 20%, 35%, and 50%, different pulse rates of 75 bpm, 100 bpm and 120 bpm, and different distances of 0 mm, 3 mm and 6 mm between stenosis and tortuosity as controlling parameters have been investigated using commercial CFD tool of Comsol in version 5.1.

2. Modelling establishment and methodology

2.1 Geometrical model and computational mesh distribution

Since the present study focuses on the blood flow in tortuous artery with stenosis, 3D geometrical models of coronary artery have been established both for curved and spiral tortuosity as shown in Fig. 1-(a) and (b). In order to ensure the geometrical independence, the artery lengths before and after tortuosity are 40mm and 50mm separately. The stenosis is located upstream the tortuosity with stenosis length of 6 mm. The horizontal length of one single curvature is 20 mm. The heights of curved and spiral tortuosity are 8 mm and 6 mm separately. The distance between stenosis and curvature as controlling parameter is named L taking the following values: 0mm, 3mm and 6mm. Comparison will be made between symmetrical and asymmetrical stenosis as

shown in Fig. 1-(c). Stenosis severity as another controlling parameter is defined as (D-d)/D*100. D is the artery diameter of 3 mm. d is the artery diameter at the narrawed site with stenosis shown in Fig. 1-(c). Different stenosis severities of 20%, 35% and 50% are studied.

[Fig. 1 near here]

In order to check the mesh independence, four mesh sizes of 210078, 570010, 1524838 and 2352717 have been studied. The WSS is investigated at these four different mesh sizes. After the third mesh size, WSS accuracy can be achieved around 2%. Taking the same way, the final determined mesh distributions can be obtained both for curved and spiral artery as shown in Fig. 2. The multigrilles method is used to generate the unstructured tetrahedral mesh elements and the average size of mesh element is 6.5e-13 m^3.

[Fig. 2 near here]

2.2. Mathematical model and boundary conditions

The blood flow is considered as incompressible and Newtonian fluid along with density of 1060 kg/m^3 and dynamic viscosity of 0.0035 Pa·s respectively [27]. Navier-stokes equations including mass conservation equation (Eq. 1) and momentum conservation equation (Eq. 2) are adopted in unsteady case. For boundary conditions, the vessel wall is considered as rigid since the diseased coronary vessels experience peak circumferential strain below 5% which makes the assumption reasonable around the plaque location [28, 29]. At the inlet, the pulsed flow at different pulse rates (bpm: beat per minute) will be imposed as shown in Fig. 3 which are reconstructed through an eight-coefficient Fourier equation (Eq. 3) and a good fitting has been achieved with the velocity profile of blood at 75 bpm [28]. According to the literature [30, 31], the

velocity profile in one cycle can be confirmed as well with pulse rate of 100 bpm and 120 bpm. At the outlet, a constant pressure of 13330 Pa is imposed [32]. The laminar blood flow is considered to be fully developed with parabolic velocity profile as Reynolds number is in the range of 90~570. The iterative methods have chosen GMRES with the maximum iteration number of 500. The time step of 0.001 s has been adopted meeting the requirement of CFL<1. The residual criteria for momentum and continuity equations is set as 10^{-5}. To make sure the periodic stability and accuracy of the results, four pulsatile cycles have been carried out. The works concerning the modelling, meshing and computing all have been done with Comsol 5.1.

$$\nabla \cdot V = 0 \tag{1}$$

$$\rho \frac{\partial V}{\partial t} + \rho V \cdot \nabla V = -\nabla p + \mu \nabla^2 V \tag{2}$$

Where V is the flow velocity, p is the pressure, ρ is the flow density and μ is the viscosity.

$$V(t) = V_0 + \sum_{n=1}^{8} V_n \cos(n\omega t) + W_n \sin(n\omega t) \tag{3}$$

Where $V_0 = \frac{1}{T}\int_0^T V(t)dt$ for $n = 0$, $V_n = \frac{2}{T}\int_0^T V(t)\cos(n\omega t)dt$ for $n \geq 1$, $W_n = \frac{2}{T}\int_0^T V(t)\sin(n\omega t)dt$ for $n \geq 1$. ω is the angular velocity.

[Fig. 3 near here]

- WSS:

$$WSS = \mu \frac{\partial u}{\partial r}\Big|_{r=r_w} \tag{4}$$

Where μ is the dynamic viscosity, u is the flow velocity in the dominant direction and r_w is the artery radius of 1.5 mm.

- TAWSS:

$$TAWSS = \frac{1}{T}\int_0^T |WSS| dt \quad (5)$$

Where T is the total time of one cycle for blood flow. TAWSS represents the shear load over time the arterial wall is subjected to and the threshold value is 0.4 Pa [33].

- Artery surface of TAWSS below 0.4 Pa (S_{TA}):

$$S_{TA} = \int_{S_T} if\,(TAWSS < 0.4,1,0) ds \quad (6)$$

Where S_T is the total surface of artery wall. The "if" function has been used in order to integrate the surface where TAWSS<0.4 Pa (=1 if so, =0 if not). Thus S_{TA} represents the surface area of potential disease sites.

3. Results analysis

3.1 Blood flow in curved artery with symmetrical and asymmetrical stenosis

Table 1 displays the TAWSS distribution for curved artery at different stenosis severities of 0%, 20%, 35% and 50% under symmetrical and asymmetrical cases at 75 bpm. In order to better understand the results analysis, some locations used in the analysis have been displayed in Fig. 4 with curved artery. It's known that TAWSS is an important WSS-based indicator to potential sites of stenosis with critical value of 0.4 Pa and lower value indicates larger possibility of plaques [33]. When we focus on the case

of 0%, it is noticed that low value regions of TAWSS are located at outer wall upstream and inner wall downstream along each curvature. As the influence of stenosis located before the tortuosity is limited to the near region of curvature, the zone in the black square is mainly focused in the subsequent analysis. TAWSS is greatly increased with larger stenosis severity both for symmetrical and asymmetrical stenosis focusing on the stenosis region and inner wall of tortuosity. The reason is the narrowed artery lumen brings more drastically varied velocity and stronger inertial force. Larger TAWSS at up wall downstream asymmetrical stenosis can be found compared to the symmetrical case. Because the geometrical change of stenosis is mainly at down wall for asymmetrical stenosis, stronger inertial force is almost remained near the up wall. Quantified results regarding the artery surface with TAWSS below 0.4 Pa (S_{TA}) have been plotted in Fig. 5 in order to better analyze the influence of stenosis severity on the potential risks of atherosclerosis. As observed that larger stenosis severity contributes to larger value of S_{TA} both for symmetrical and asymmetrical cases. Moreover, asymmetrical stenosis tends to more risky with larger value of S_{TA} compared to symmetrical case. The reason is that asymmetrical stenosis brings more disturbed flow downstream the stenosis due to the uneven effects on the arterial wall radially compared to the symmetrical stenosis.

[Table 1 near here]

[Fig. 4 near hear]

[Fig. 5 near hear]

Physical activities of patients are closely related to the hemodynamic variation through changed flow pattern [9]. Thus, the TAWSS distribution is also studied at different pulse rates of 75 bpm, 100 bpm and 120 bpm with symmetrical and asymmetrical

stenosis of 35% as shown in Table 2. Even though the changed pulse rate will bring hemodynamic variation overall the artery, in order to be consistent to the analysis above we still mainly focus on the stenosis part and the near part of tortuosity. As can be seen that larger pulse rate greatly increases the TAWSS value and low TAWSS regions located right downstream the stenosis and at the outer wall of tortuosity are both decreased because of the more sharply varied velocity pattern. The quantified comparisons between symmetrical and asymmetrical stenosis regarding arterial surface area of TAWSS below 0.4 Pa affected by different pulse rates are shown in Fig. 6 which has well confirmed the observations in Table 2. The obviously negative relationship between S_{TA} and pulse rate has been proved and a larger value of S_{TA} at asymmetrical case can be always observed.

[Table 2 near here]

[Fig. 6 near hear]

Following the effect of stenosis severities and pulse rates on hemodynamic variation, the influence of distance between stenosis and tortuosity is discussed as well. Similarly, Table 3 shows the TAWSS distribution at different distances of 0 mm, 3 mm and 6 mm between stenosis and tortuosity with symmetrical and asymmetrical stenosis of 35% at 75 bpm. As can be seen, the increased distance between stenosis and tortuosity contributes to lower value of TAWSS especially when we focus on the inner wall of tortuosity and the reduction of TAWSS is more obvious for symmetrical case. The increased distance in our case tends to increase the low value regions of TAWSS. Compared to the symmetrical stenosis, larger value of TAWSS can be got at up wall after asymmetrical stenosis because there is no geometrical change along up wall. Similarly, the corresponding quantified analysis has been made with Fig. 7 investigating

the effects of distances between stenosis and tortuosity on the surface area of TAWSS below 0.4 Pa for symmetrical and asymmetrical cases. It is displayed that the value of S_{TA} is increased in asymmetrical case with the increasing of distance between stenosis and tortuosity. However, for symmetrical case, the value of S_{TA} is decreased with distance increased from 3 mm to 6 mm. The reason is that the flow after stenosis is still not be able to fully developed with effects of the formed recirculation downstream the asymmetrical stenosis and tortuosity. However, for symmetrical stenosis, the flow has been recovered to be fully developed when the distance is 6 mm. The larger value of S_{TA} at symmetrical case has been observed compared to the asymmetrical case with the increased distance of 3 mm and 6 mm which is in contrast to the results with effects of stenosis severity and pulse rate. For the reason, it is because the increased distance between stenosis and tortuosity leads to more low value region for the symmetrical case compared to the asymmetrical case which can balance and even over the effect of stenosis geometrical characteristics.

[Table 3 near here]

[Fig. 7 near hear]

In order to check out the flow variations, two cross sections S1 and S2 are selected as shown in Fig. 8. The streamlines and velocity distribution on these two cross sections are studied at different stenosis severities as shown in Table 4. When focusing on S1 in Table 4, it is found that the high value region of velocity corresponds to the stenosis throat region and higher velocity value is positively related to larger stenosis severity both for symmetrical and asymmetrical cases. The streamlines are more disturbed with increased stenosis severity especially for symmetrical case even though there is no vortice formed. However, when focusing on S2 both in symmetrical and asymmetrical

cases, there is no big changes occurred to the peak value of velocity distribution with the increased stenosis severity. The streamlines on S2 is more significantly disturbed compared to S1 especially for asymmetrical case. The vortices can be observed and the vortice number is developed from 2 into 4 with increased stenosis severity. Compared to symmetrical case, asymmetrical stenosis contributes to stronger flow disturbance at the same stenosis severity. Similar phenomena can be found out with the effects of different pulse rates and distances between stenosis and tortuosity which are not shown here. The vortices are commonly found at S2 where the flow tend to be more disturbed with larger pulse rate and smaller distance especially in asymmetrical case.

[Fig. 8 near here]

[Table 4 near here]

3.2 Blood flow in spiral artery with symmetrical and asymmetrical stenosis

As spiral tortuosity is one of the existing arterial morphological states found in human body, it is necessary to study how the hemodynamics are affected by spiral non-planar structure of artery instead of curved planar structure. Similarly, some location definitions used in analysis have been shown in Fig. 9. Table 5 shows the TAWSS distribution with symmetrical and asymmetrical stenosis of 0%, 20%, 35% and 50% at 75 bpm for the spiral artery. The results are displayed from front and back views. When focusing on the case of 0%, it is found that low value of TAWSS is mainly located at entry and exit parts of the tortuosity. Along the tortuous segment, larger value of TAWSS is always found at outer wall compared to the inner wall. Since the effect of stenosis is limited to the near region, in the following analysis the region in black square is mainly focused. With the increasing of stenosis severity, the high value region of TAWSS is greatly increased. The low value region of TAWSS is found to be mainly

located downstream the stenosis both in front view and back view. Quantified analysis has been followed with Fig. 10 which evaluates the surface area of TAWSS below 0.4 Pa under different stenosis severities for symmetrical and asymmetrical cases. Larger value of S_{TA} can be found mainly in the symmetrical case compared to the asymmetrical case. The positive relationship between S_{TA} and stenosis severity found in curved artery has been disturbed with increased stenosis severity of 50% in spiral artery.

[Fig. 9 near here]

[Table 5 near here]

[Fig. 10 near hear]

Table 6 shows TAWSS distribution at different pulse rates for symmetrical and asymmetrical stenosis of 35% for spiral artery. Larger pulse rate leads to overall increased TAWSS because of the increased velocity variation near wall. The low value region downstream the stenosis is decreased at both front and back views with increased pulse rate. The corresponding quantified analysis has been made in Fig. 11 where the surface area of TAWSS below 0.4 Pa at different pulse rates has been plotted for the cases of symmetrical and asymmetrical stenosis. The negative relationship between S_{TA} and pulse rate can be observed and the larger value of S_{TA} is obtained with symmetrical stenosis compared to the asymmetrical stenosis.

[Table 6 near here]

[Fig. 11 near hear]

As the stenosis is located at the non-tortuous segment before the spiral tortuosity, the distance between stenosis and spiral tortuosity need to be considered. Table 7 shows the TAWSS distribution at different distances of 0 mm, 3 mm and 6 mm between stenosis

and tortuosity for symmetrical and asymmetrical stenosis of 35% at 75 bpm. larger distance between stenosis and tortuosity greatly increases the low value region of TAWSS either at front view or back view. Compared to the asymmetrical stenosis case, larger low value region of TAWSS is observed at symmetrical case in the artery segment between stenosis and toruosity. The reason is that asymmetrical stenosis geometry can more maintain the inertial force after the stenosis site within regions where the original artery geometry is remained. Fig. 12 shows the surface area of TAWSS below 0.4 Pa at different distances and confirmed the observations from Table 7. The value of S_{TA} is greatly increased with larger distance between stenosis and tortuosity as the flow is not able to be fully developed affected by the spiral tortuosity.

[Table 7 near here]

[Fig. 12 near hear]

Spiral tortuosity as non-planar geometry makes the flow disturbance is more complicated. Compared to the curved tortuosity, both vertical and lateral curvature variations affect the blood flow for spiral artery instead of only vertical curvature variation. Thus the flow streamlines are studied in view of 3D instead of the 2D cross section compared to the planar curved artery. As shown in Table 8, streamlines colored with velocity around stenosis and tortuosity have been studied at different stenosis severities. Flow disturbance downstream stenosis and streamlines moving forward spirally along the tortuosity can be easily observed. The peak value of velocity can be obtained at the stenosis site both in symmetrical and asymmetrical cases affected by the reduced artery diameter and the peak value is increased with larger stenosis severity. Moreover, with the increasing of stenosis severity, the flow disturbance is more complicated especially at stenosis of 50% and the recirculation downstream stenosis is

more clearly observed. Compared to symmetrical case, the formation of recirculation downstream the stenosis in asymmetrical case is more obvious which is affected by the stenosis height. Similarly, the increased pulse rate and distance contribute to more disturbed flow and recirculation formation as well, especially in asymmetrical case which are not shown here.

[Table 8 near here]

4. Discussion

This present study has provided us an insight for the influences of planar and non-planar arterial tortuosity in the potential risks of plaque generation coupling the existence of stenosis. Besides the qualitative analysis of hemodynamics as commonly conducted in the existing literature [10, 12, 21], the quantitative analysis of disease onset area is employed strictly following the critical value of evaluation. As described above, both curved and spiral arteries with symmetrical and asymmetrical stenosis have been established in order to investigate the flow disturbance and hemodynamic variations inside separately. As observed through the results, TAWSS distribution tends to be symmetrical through a 2D section in curved artery which is consistent with the works of Liu et al. [22], however, the TAWSS distribution in spiral artery is more complex affected by the non-planar tortuosity structure. The low value region of TAWSS has been focused and pointed out to specify the potential sites of plaque generation. When focusing on the non-tortuous segment, low value region of TAWSS can be always found downstream the stenosis both for curved and spiral artery. Consistently, both in-vivo and in-vitro works have proved the local platelet aggregation downstream the stenotic site [34, 35]. Along the curved tortuosity, the low value region of TAWSS has been observed at the outer wall upstream and inner wall downstream for each curvature as shown in Table 1 which is enforced by the direction of centrifugal force. Along spiral

tortuous segment, the low value region of TAWSS is prone to be always located at the inner wall as shown in Table 5 which is determined by the more complicated tortuosity structure and the more irregular alterations of centrifugal force direction.

Stenosis located at the non-tortuous segment before the tortuosity is considered following the recent clinical findings [25]. Thus the distance between stenosis and tortuosity as a controlling parameter has been put forward and investigated in our study as well as different pulse rates and stenosis severities. The results revealed that larger risks of atherosclerosis generally go with larger stenosis severity, smaller pulse rate and larger distance between stenosis and tortuosity. However, some exceptions have been observed with the cases of symmetrical stenosis in curved artery with distance of 6 mm and stenosis severity of 50% in spiral artery. This is due to the fully developed blood flow after the stenosis site in the case of symmetrical case in curved artery with increased distance of 6 mm. For spiral artery, when the stenosis severity is increased to 50%, the low value region of TAWSS will be greatly reduced and restricted by the spiral tortuosity structure. Regarding the comparisons between symmetrical and asymmetrical stenosis, it is found that the value of S_{TA} tends to be higher for asymmetrical stenosis compared to symmetrical stenosis for curved artery under the effects of stenosis severity and pulse rate. The reason is that asymmetrical stenosis brings more disturbed flow downstream the stenosis due to the uneven effects on the arterial wall radially compared to the symmetrical stenosis. However, the increased distance between stenosis and tortuosity leads to more low value region of TAWSS especially for the symmetrical case compared to the asymmetrical case which can balance and even over the effect of stenosis geometrical characteristics. The peak inertial force tends to the less narrowed side of vessel wall leading to larger TAWSS at up wall in asymmetrical case instead of comparatively even distribution of smaller

TAWSS in symmetrical case. In spiral artery, larger value of S_{TA} can be always found in the case of symmetrical stenosis compared to the asymmetrical stenosis. The effects of asymmetrical stenosis have been totally disturbed and weakened by the spiral tortuosity with more complicated geometrical variations.

The vortices indicating the flow disturbance level have been found affected by the curvature, and the streamlines moving forward spirally along the spiral tortuosity can be easily observed affected by the spiral structure. It is notable that when we compare the values of S_{TA} between curved and spiral tortuosities through Fig. 5-7 and Fig. 10-12 respectively, the obviously smaller values have been obtained under different conditions for spiral artery. This finding is consistent with the investigations by the group of X. Deng et al. [36, 37]: swirling/spiral flows could suppress platelet adhesion. G. De Nisco et al. has demonstrated the atheroprotective nature of helical flow and the helicity intensity inversely associated with the unfavorable condition of WSS [38, 39]. Clinical study conducted by J.G. Houston et al. has concluded as well that spiral flow is beneficial to inhibit the suspected artery stenosis [40].

5. **Limitations**

In the present study, there are some limitations with the established model. The geometrical model of coronary artery is established as a cylinder which is idealized compared to the reality. Thus the patient-specific artery with stenosis and tortuosity need to be further considered into the model closer to the practice. The heart curvature which is much smaller compared to the tortuousity curvature has been neglected. Referring to the literature [41], a good agreement on the average WSS has been demonstrated between rigid and deformable vessels. Thus a rigid and no-slip coronary artery wall has been set in this study and the heart movement has been ignored. As

several experimental works [42, 43] have confirmed the multicomponent nature of blood, multi-phase approach should be further considered for modeling of blood instead of single phase in this study.

6. Conclusion

The present study investigates the flow topology and hemodynamic variations in coronary artery of two different morphological characteristics: curved and spiral tortuosity, coupling the existence of symmetrical and asymmetrical stenosis before these tortuosities. The results reveal that low value of TAWSS located downstream the stenosis can be observed. Along curved tortuosity, the low value region of TAWSS is located outer wall upstream and inner wall downstream for each curvature. However, the smaller value of TAWSS tends to be always located at inner wall along the spiral tortuosity. Larger area of TAWSS below 0.4 Pa goes with larger stenosis severity, smaller pulse rate and larger distance between stenosis and tortuosity both for curved and spiral artery except in the cases of symmetrical stenosis in curved artery with distance of 6 mm and stenosis severity of 50% in spiral artery. The value of s_{TA} tends to be higher for asymmetrical stenosis compared to symmetrical stenosis within the effect of stenosis sevetrity and pulse rate which can be reversed by increasing the distance between stenosis and tortuosity for curved artery. However, for spiral artery the higher value of s_{TA} always goes with symmetrical stenosis compared to asymmetrical stenosis. Smaller s_{TA} can be observed in spiral artery compared to the curved artery at the same condition. Meanwhile the flow disturbance tends to be stronger with larger stenosis severity and pulse rate, and smaller distance between stenosis and tortuosity especially for asymmetrical stenosis in curved artery. Flow disturbance downstream stenosis and streamlines moving forward spirally along the tortuosity can be easily

observed in spiral artery.

Conflict of interest statement

None declared

References

[1] Gupta A, Panda P, Sharma Y, Mahesh, A, Sharma P, Mahesh NK. Clinical profile of patients with coronary tortuosity and its relation with coronary artery disease. Int J Cardiovasc Res 2018; 4(2): 66-71.

[2] Van Dalen BM, Tzikas A, Soliman OII, Kauer F, Heuvelman HJ, Vletter WB, Geleijnse ML. Left ventricular twist and untwist in aortic stenosis. Int J Cardiol 2011; 148(3): 319–324.

[3] Razavi A, Shirani E, Sadeghi MR. Numerical simulation of blood pulsatile flow in a stenosed carotid artery using different rheological models. J Biomech 2011; 44: 2021-2030.

[4] Long Q, Xu XY, Ramnarine KV, Hoskins P. Numerical investigation of physiologically realistic pulsatile flow through arterial stenosis. J Biomech 2001, 34: 1229-1242.

[5] Foong LK, Zarringhalam M, Toghraie D, Izadpanahi N, Yan SR, Rostami S. Numerical study for blood rheology inside an artery: The effects of stenosis and radius on the flow behavior. Comput Meth Prog Bio 2020; 193: 105457.

[6] Yan SR, Zarringhalam M, Toghraie D, Foong LK, Talebizadehsardari P. Numerical investigation of non-Newtonian blood flow within an artery with cone shape of stenosis in various stenosis angle. Comput Meth Prog Bio 2020; 192: 105434.

[7] Akbar NR, Non-Newtonian model study for blood flow through a tapered artery with a stenosis. Alex Eng J 2016; 55: 321-329.

[8] Sood T, Roy S, Pathak M. Effect of pulse rate variation on blood flow through axisymmetric and asymmetric stenotic artery models. Math Biosci 2018; 298: 1-18.

[9] Khosravani-Rudpishi M, Joharimoghadam A, Rayzan E. The significant coronary tortuosity and atherosclerotic coronary artery disease; What is the relation? J Cardiovasc Thorac Res 2018; 10(4): 209-21.

[10] Zhang C, Xie S, Li S, Pu F, Deng X, Fan Y, Li D. Flow patterns and wall shear stress distribution in human internal carotid arteries: the geometric effect on the risk for stenoses. J Biomech 2012; 45(1):83-9.

[11] Qiao AK, Guo XL, Wu SG, Zeng YJ, Xu XH. Numerical study of nonlinear pulsatile flow in S-shaped curved arteries. Med Eng Phys 2004; 26(7):545-52.

[12] Xie X, Wang Y, Zhu H, Zhou J. Computation of hemodynamics in tortuous left coronary artery: a morphological parametric study. J Biomech Eng 2014. 136(10): 101006.

[13] Jarrahi M, Castelain C, Peerhossaini H. Laminar sinusoidal and pulsatile flows in a curved pipe. J appl fluid mech 2011; 4: 21-26.

[14] Najjari MR, Plesniak MW. Evolution of vortical structures in a curved artery model with non-Newtonian blood-analog fluid under pulsatile inflow conditions. Exp Fluids 2016; 57(6): 100.

[15] Siggers JH, Waters SL. Steady flows in pipes with finite curvature. Phys Fluids 2005; 17: 1–18.

[16] Shahcheraghi N, Dwyer HA, Cheer AY, Barakat AI, Rutaganira T. Unsteady and three-dimensional simulation of blood flow in the human aortic arch. J Biomech Eng 2002; 124: 378.

[17] Dash RK, Jayaraman G, Mehta KN. Flow in a catheterized curved artery with stenosis. J Biomech 1999; 32: 49-61.

[18] Wang L, Zhao F, Wang DM, Hu S, Liu JC, Zhou ZL, Lu J, Qi P, Song SY. Pressure drop in tortuosity/kinking of the internal carotid artery: simulation and clinical investigation. BioMed Research International 2016; 2016: 1-8.

[19] Santamarina A, Weydahl E, Siegel J, Moore J. Computational analysis of flow in a curved tube model of the coronary arteries: effects of time-varying curvature. Ann Biomed Eng 1998; 26 (6): 944-954.

[20] Xie X, Wang Y, Zhou H. Impact of coronary tortuosity on the coronary blood flow: a 3D computational study. J Biomech 2013; 46(11): 1833–1841.

[21] Buradi A, Mahalingam A. Impact of coronary tortuosity on the artery hemodynamics. Biocybern Biomed Eng 2020; 40: 126-147.

[22] Liu GY, Wu J, Huang W, Wu W, Zhang H, Wong KKL, Ghista DN. Numerical simulation of flow in curved coronary arteries with progressive amounts of stenosis using fluid-structure interaction modelling. J Med Imaging Health Inform 2014; 4(4):605-11.

[23] Liu B. The influences of stenosis on the downstream flow pattern in curved arteries. Med Eng Phys 2007; 29: 868-876.

[24] Biglarian M, Larimi MM, Afrouzi HH, Moshfegh A, Toghraie D, Javadzadegan A, Rostami S. Computational investigation of stenosis in curvature of coronary artery within both dynamic and static models. Comput Meth Prog Bio 2020; 185: 105170.

[25] Li Y, Feng Y, Ma GS, Shen CX, Liu NF. Coronary tortuosity is negatively correlated with coronary atherosclerosis. J Int Med Res 2018; 46(12): 5205–5209.

[26] Han HC. Twisted blood vessels: symptoms, etiology and biomechanical mechanisms. J Vasc Res 2012; 49: 185 - 197.

[27] Gundelwein L, Miro J, Gonzalez BF, Lapierre C, Rohr K, Duoong L. Personalized stent design for congenital heart defects using pulsatile blood flow simulations. J Biomech 2018; 81: 68–75.

[28] Chabi F, Champmartin S, Sarraf Ch, Noguera R. Critical evaluation of three hemodynamic models for the numerical simulation of intra-stent flows. J Biomech 2015; 48(10): 1769–1776.

[29] Kelle S, Hays AG, Hirsch GA, Gerstenblith G, Miller JM, Steinberg AM, Schär M, Texter JH, Wellnhofer E, Weiss RG, Stuber M. Coronary artery distensibility assessed by 3.0 Tesla coronary magnetic resonance imaging in subjects with and without coronary artery disease. Am J Cardio 2011; 108: 491-7.

[30] Heusch G. Heart rate in the pathophysiology of coronary blood flow and myocardial ischaemia: benefit from selective bradycardic agents. Br J Pharmacol 2008; 153: 1589-1601.

[31] Kim HJ, Vignon-Clementel IE, Figueroa CA, Jansen KE, Taylor CA. Developing computational methods for three-dimensional finite element simulations of coronary blood flow. Finite Elem Anal Des 2010; 46: 514-525.

[32] Gudiño E, Sequeira A. 3D mathematical model for blood flow and non-Fickian mass transport by a coronary drug-eluting stent. Appl Math Model 2017; 46: 161-180.

[33] Malek AM, Alper SL, Izumo S. Hemodynamic shear stress and its role in atherosclerosis. J Am Med Assoc 1999; 282: 2035-2042.

[34] Tricot O, Mallat Z, Heymes C, Belmin J, Lesèche G, Tedgui A. Relation between endothelial cell apoptosis and blood flow direction in human atherosclerotic plaques. Circulation 2000; 101: 2450-3.

[35] Westein E, van der Meer AD, Kuijpers MJ, Frimat JP, van den Berg A, Heemskerk JW. Atherosclerotic geometries exacerbate pathological thrombus formation poststenosis in a von Willebrand factor-dependent manner. Proc Natl Acad Sci U S A 2013; 110: 1357-62.

[36] Zhan F, Fan Y, Deng X. Effect of swirling flow on platelet concentration distribution in small-caliber artificial grafts and end-to-end anastomoses. Acta Mech Sin 2011; 27: 833-839.

[37] Sun A, Fan Y, Deng X. Intentionally induced swirling flow may improve the hemodynamic performance of coronary bifurcation stenting. Catheter Cardiovasc Interv 2012; 79: 371–377.

[38] De Nisco G, Kok AM, Chiastra C, Gallo D, Hoogendoorn A, Migliavacca F, Wentzel JJ, Morbiducci U. The Atheroprotective Nature of Helical Flow in Coronary Arteries. Ann Biomed Eng 2018; 2: 425-438.

[39] De Nisco G, Hoogendoorn A, Chiastra C, Gallo D, Kok AM, Morbiducci U, Wentzel JJ. The impact of helical flow on coronary atherosclerotic plaque development. Atherosclerosis 2020; 300: 39-46.

[40] Houston JG, Gandy SJ, Milne W, Dick JB, Belch JJ, Stonebridge PA. Spiral laminar flow in the abdominal aorta: a predictor of renal impairment deterioration in patients with renal artery stenosis? Nephrol Dial Transplant 2004; 19:1786-1791.

[41] Siogkas E, Sakellarios A, Exaechos T, Parodi O. Blood flow in arterial segments: rigid vs. deformable walls simulationsn. J Serb Soc Comput Mech 2011; 5: 69-77.

[42] Haynes RH. Physical basis of the dependence of blood viscosity on tube radius. Am J Physiol-Legacy Content 1960; 198: 1193-1200.

[43] Stadler AA, Zilow EP, Linderkamp O. Blood viscosity and optimal hematocrit in narrow tubes. Biorheology 1990; 27: 779-788.

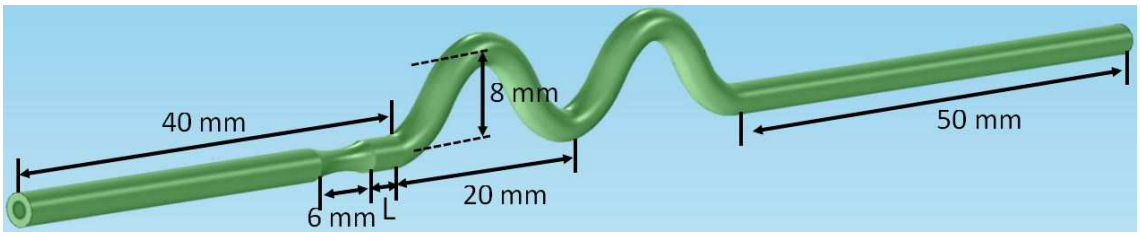

(a) Curved artery with stenosis

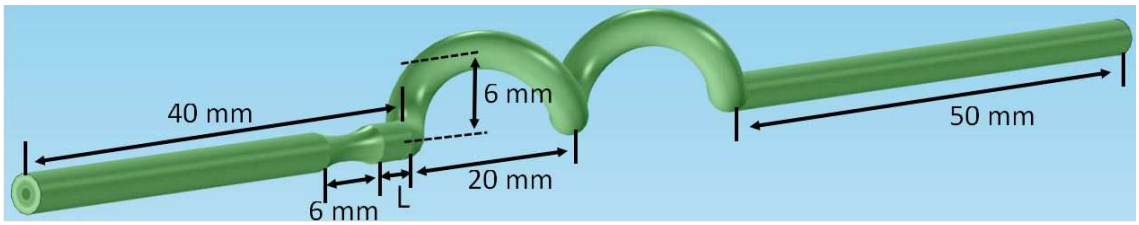

(b) Spiral artery with stenosis

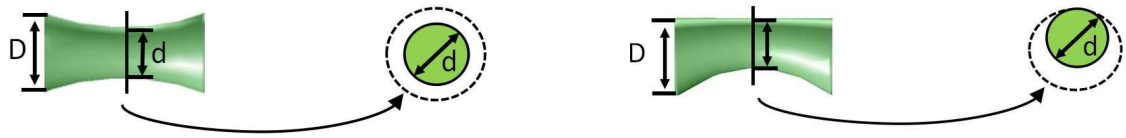

Symmetrical stenosis Asymmetrical stenosis

(c) Structure of symmetrical and asymmetrical stenosis

Fig. 1. 3D geometrical model of curved artery (a) and spiral artery (b) with stenosis of symmetrical and asymmetrical structure (c).

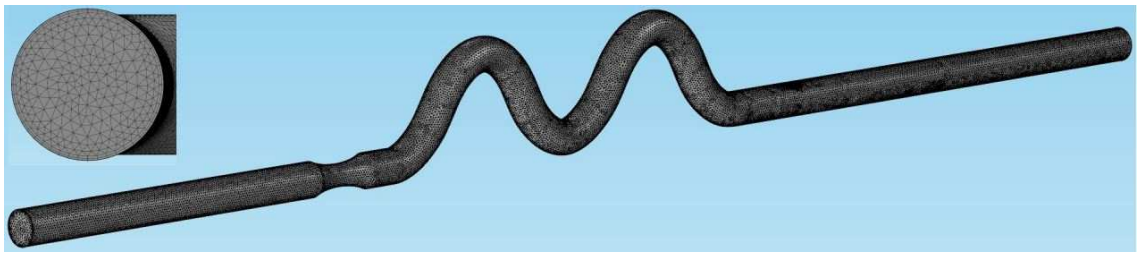

(a) Curved artery

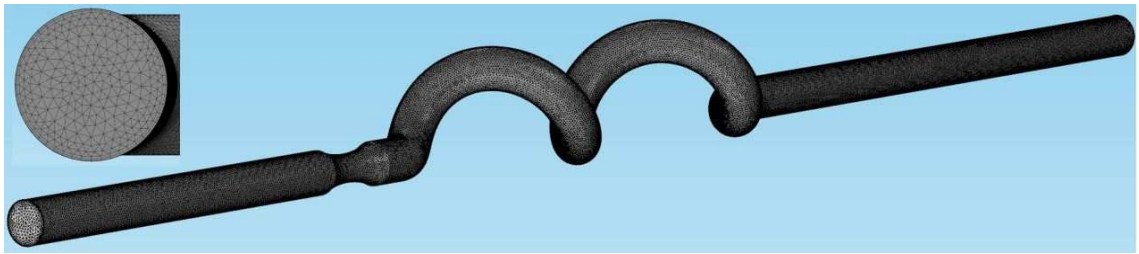

(b) Spiral artery

Fig. 2. Computational mesh for curved artery (a) and spiral artery (b).

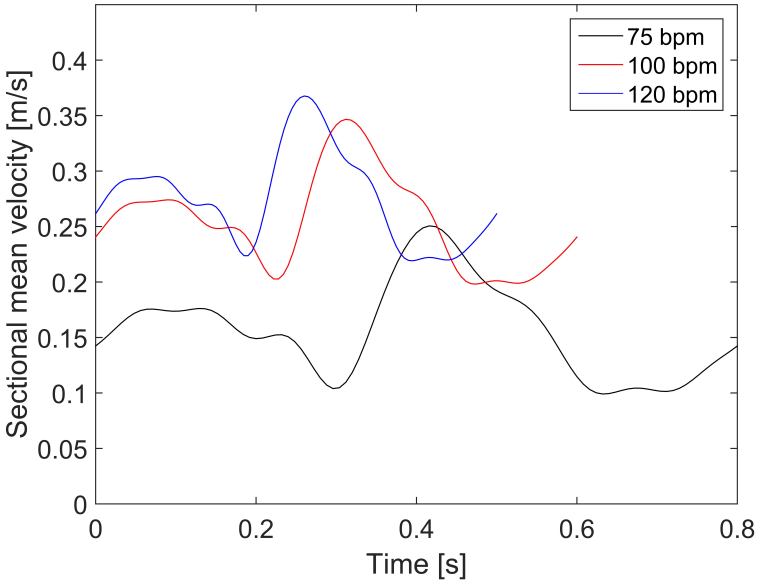

Fig. 3. Inlet pulsed flow in one cycle at different pulse rates.

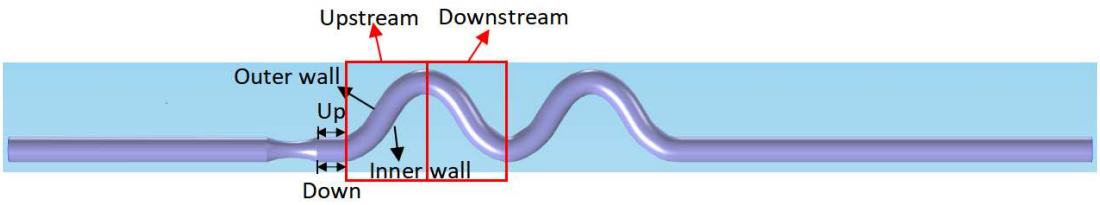

Fig. 4. Location definitions with curved artery coupling stenosis.

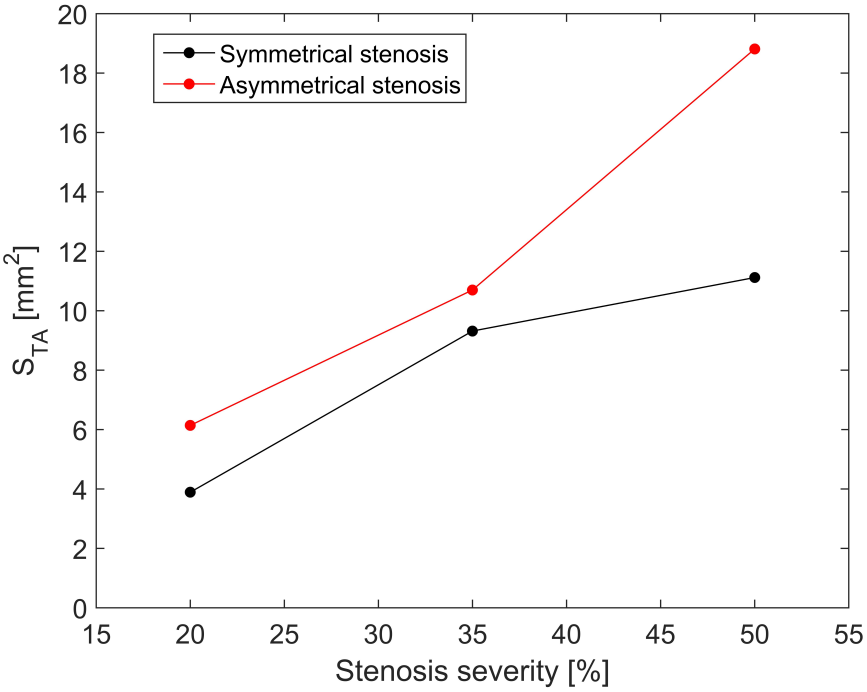

Fig. 5. Artery surface of TAWSS below 0.4 Pa at different stenosis severities for curved artery.

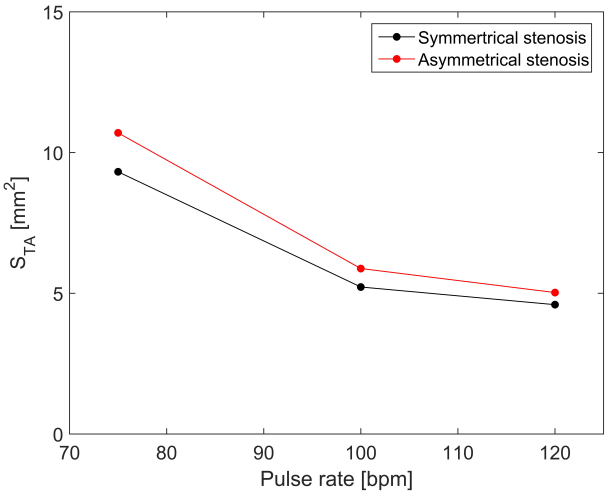

Fig. 6. Artery surface of TAWSS below 0.4 Pa at different pulse rates for curved artery.

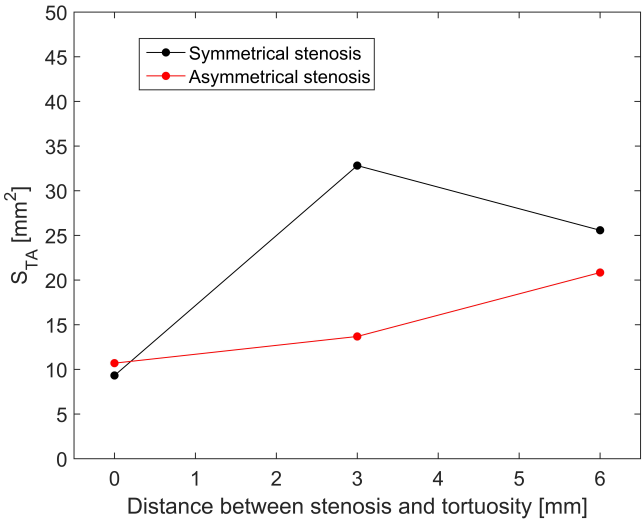

Fig. 7. Artery surface of TAWSS below 0.4 Pa at different distances between stenosis and tortuosity for curved artery.

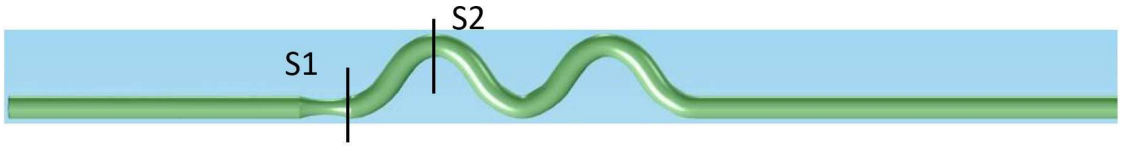

Fig. 8. Positions of cross section selection.

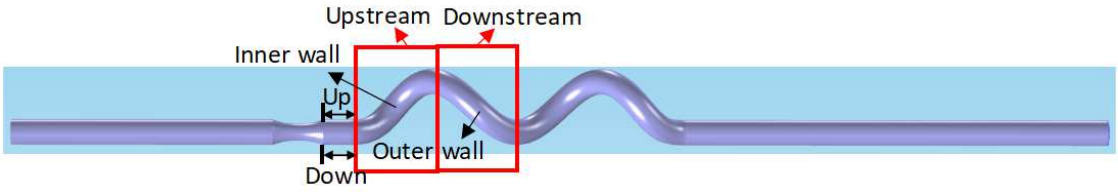

Fig. 9. Location definitions with spiral artery coupling stenosis.

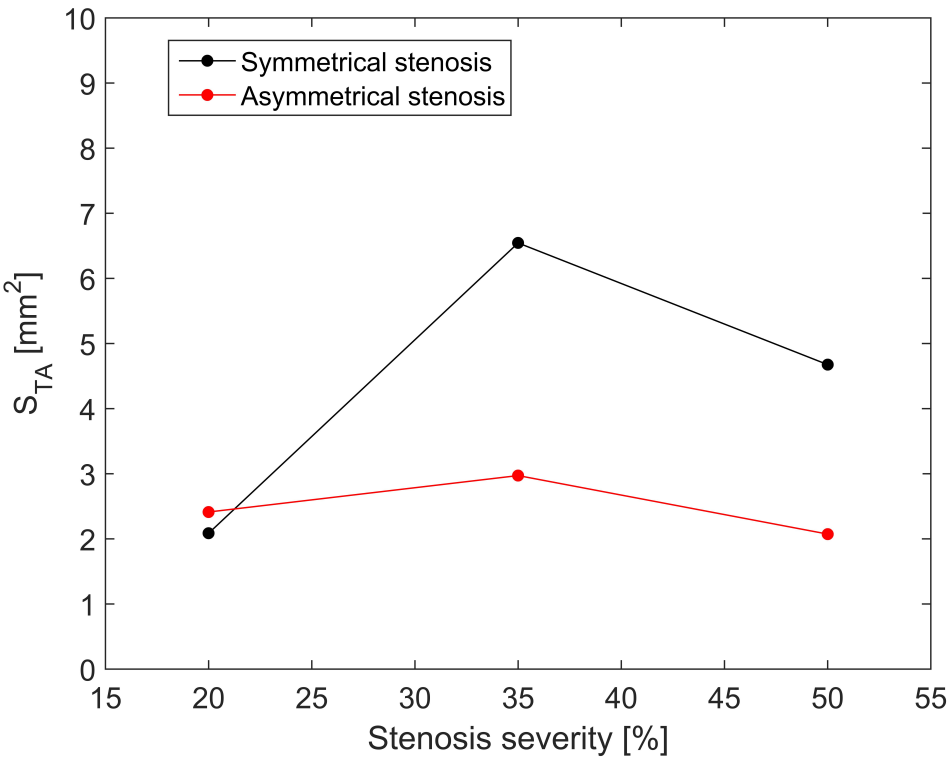

Fig. 10. Artery surface of TAWSS below 0.4 Pa at different stenosis severities for spiral artery.

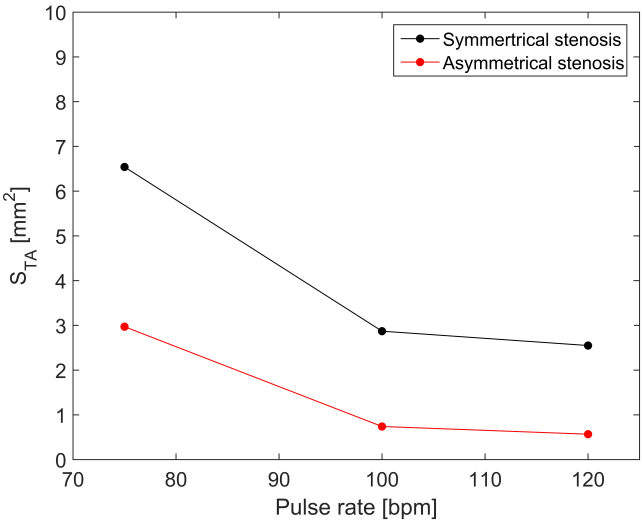

Fig. 11. Artery surface of TAWSS below 0.4 Pa at different pulse rates for spiral artery.

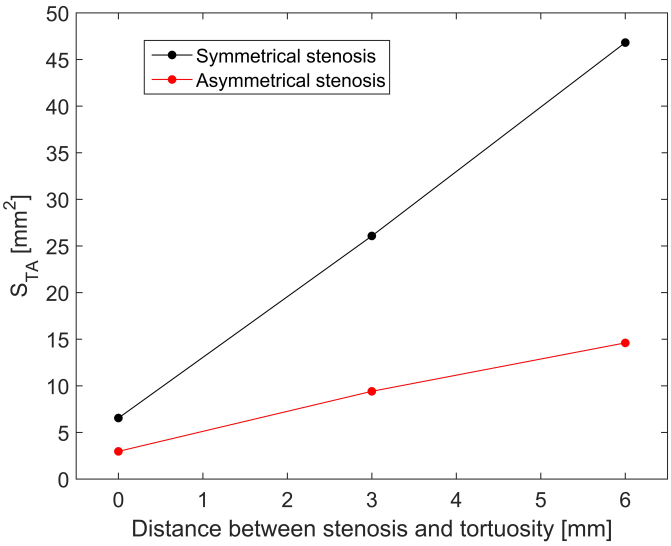

Fig. 12. Artery surface of TAWSS below 0.4 Pa at different distances between stenosis and tortuosity for spiral artery.

Table 1. TAWSS distribution at different stenosis severities for curved artery with symmetrical and asymmetrical stenosis at 75 bpm.

Diameter stenosis	Symmetrical stenosis	Asymmetrical stenosis
0%	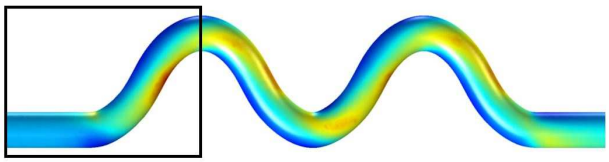	
20%	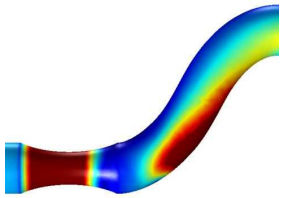	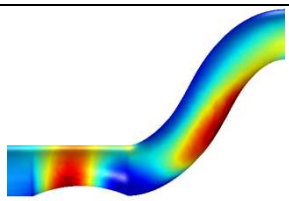
35%	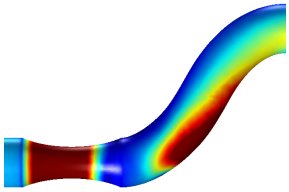	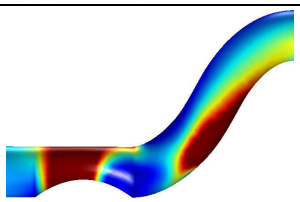
50%	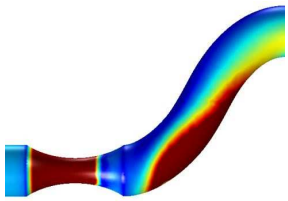	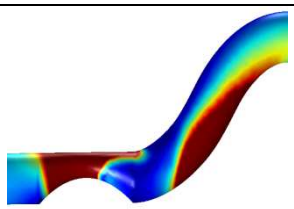
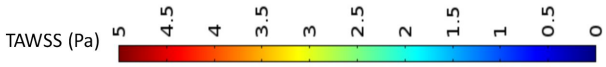		

Table 2. TAWSS distribution at different pulse rates for curved artery with symmetrical and asymmetrical stenosis of 35%.

Pulse rate	symmetrical	asymmetrical
75 bpm	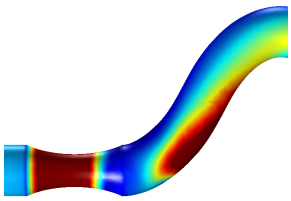	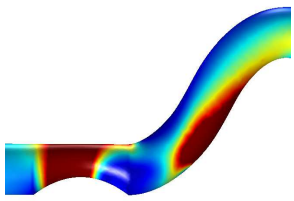
100 bpm	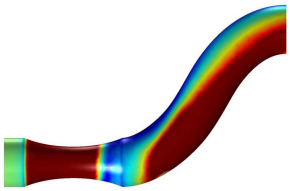	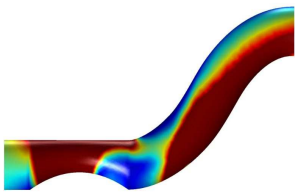
120 bpm	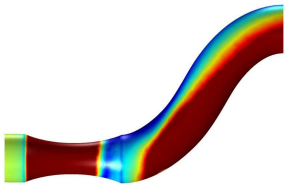	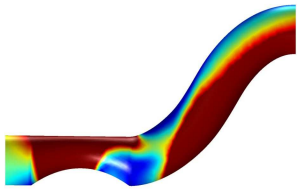
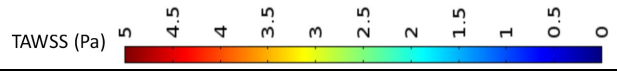		

Table 3. TAWSS distribution at different distances between stenosis and toruosity for curved artery with symmetrical and asymmetrical stenosis of 35% at 75 bpm.

Distance	Symmetrical	Asymmetrical
0mm	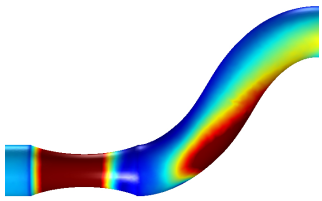	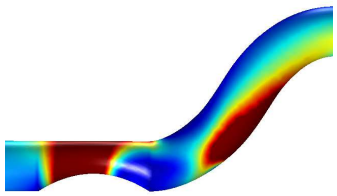
3mm	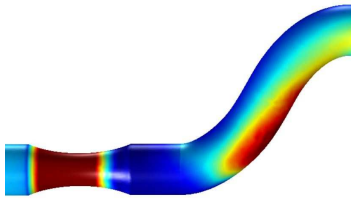	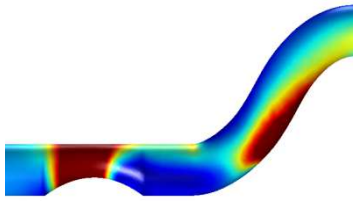
6mm	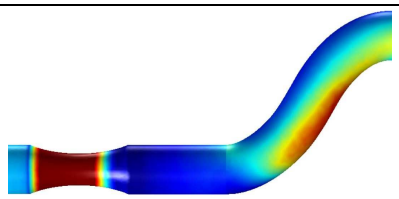	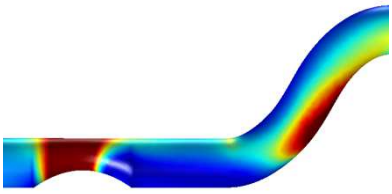
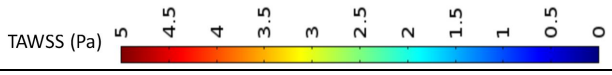		

Table 4. Streamlines with colored velocity distribution and vectors at S1 and S2 for in curved artery of different symmetrical and asymmetrical stenosis at 75 bpm at T/2.

Stenosis severity	Symmetrical stenosis		Asymmetrical stenosis	
	S1	S2	S1	S2
20%	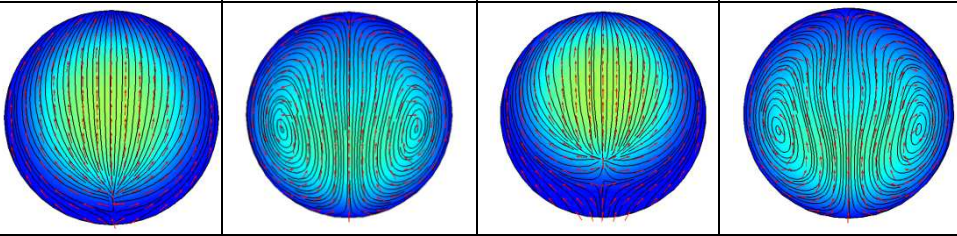			
35%	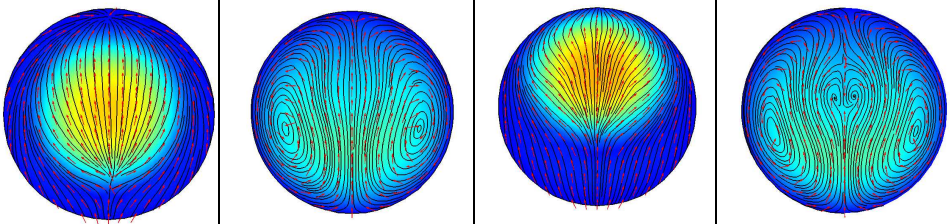			
50%	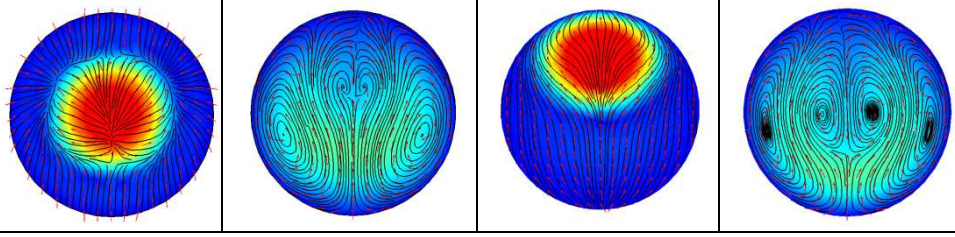			
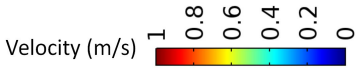				

Table 5. TAWSS distribution at different stenosis severities for spiral artery with symmetrical and asymmetrical stenosis at 75 bpm.

Diameter stenosis	View	Symmetrical stenosis	Asymmetrical stenosis
0%	front	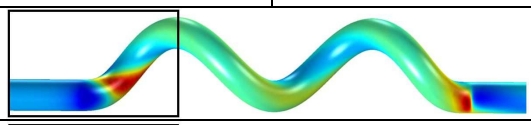	
	back	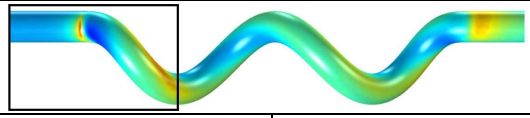	
20%	front	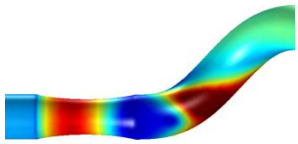	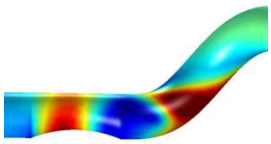
	back	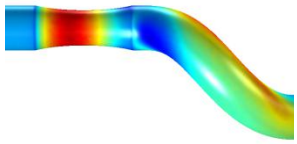	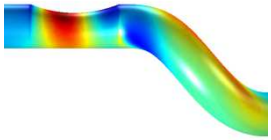
35%	front	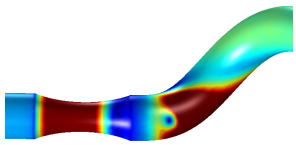	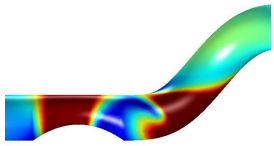
	back	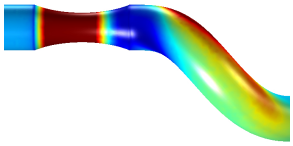	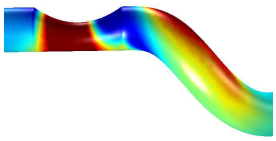
50%	front	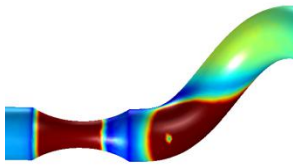	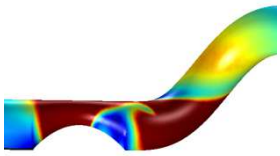
	back	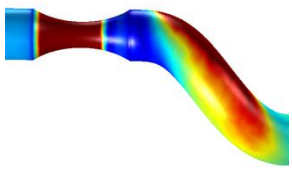	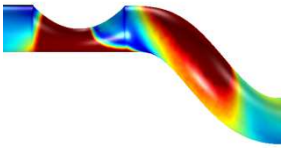
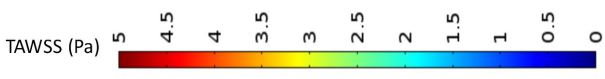			

Table 6. TAWSS distribution at different pulse rates for spiral artery with symmetrical and asymmetrical stenosis of 35%.

Pulse rate	View	Symmetrical stenosis	Asymmetrical stenosis
75 bpm	front	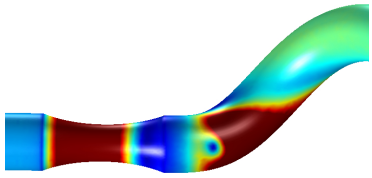	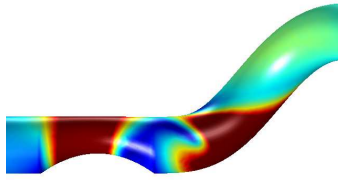
	back	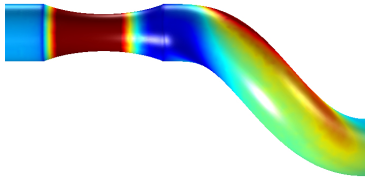	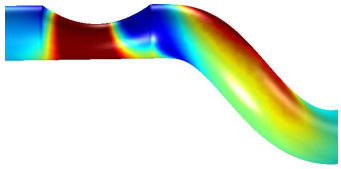
100 bpm	front	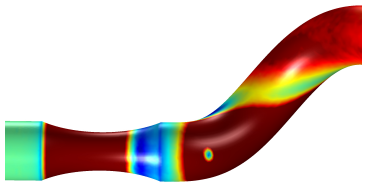	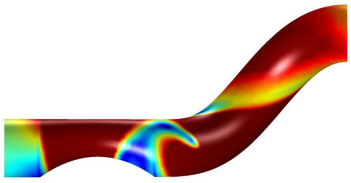
	back	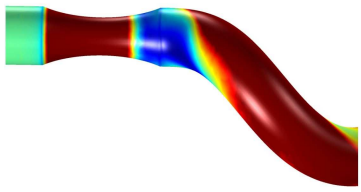	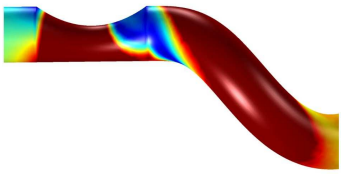
120 bpm	front	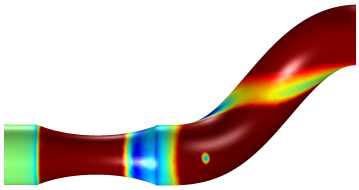	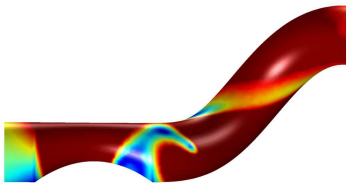
	back	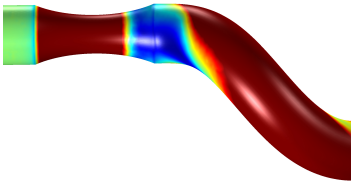	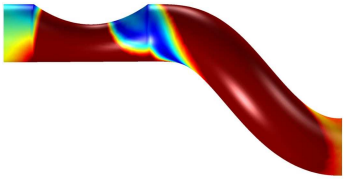
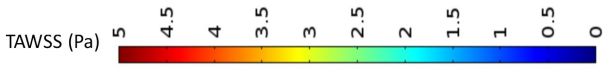			

Table 7. TAWSS distribution at different distances between stenosis and tortuosity for spiral artery with symmetrical and asymmetrical stenosis of 35% at 75 bpm.

Distance	View	Symmetrical stenosis	Asymmetrical stenosis
0 mm	front	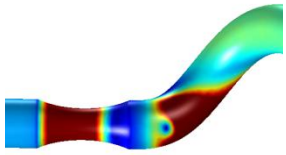	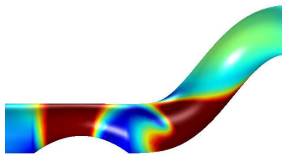
	back	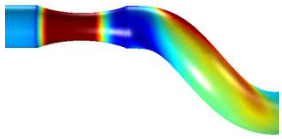	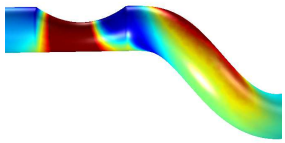
3 mm	front	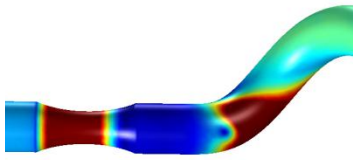	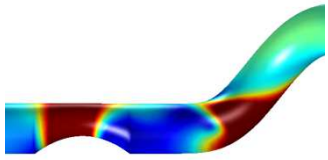
	back	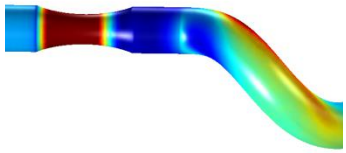	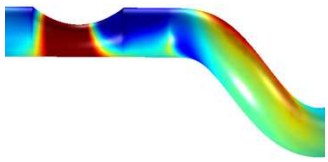
6 mm	front	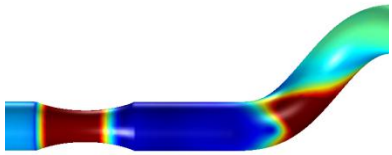	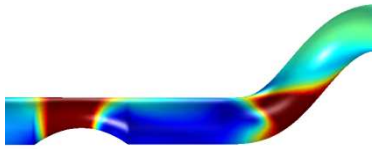
	back	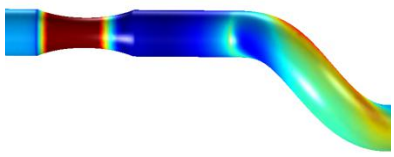	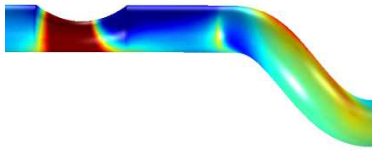
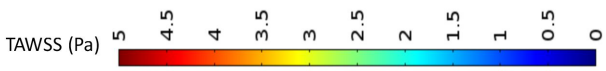			

Table 8. Streamlines at different stenosis severities for spiral artery with symmetrical and asymmetrical stenosis at 75 bpm at T/2.

Stenosis severity	Symmetrical stenosis	Asymmetrical stenosis
20%		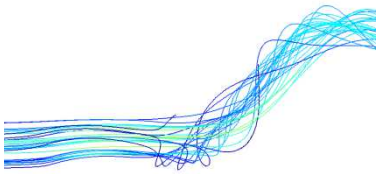
35%	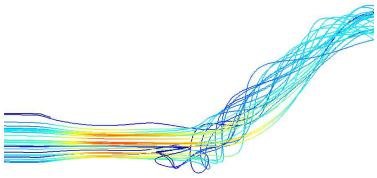	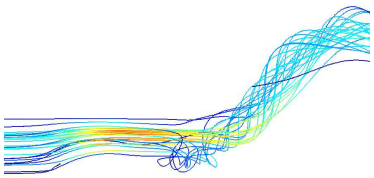
50%